2008

Serendipitous Chandra X-ray Detection of a Hot Bubble within the Planetary Nebula NGC 5315

Joel H. Kastner
Rochester Institute of Technology

Rodolfo Montez Jr
Rochester Institute of Technology

Bruce Balick
University of Washington

Orsola De Marco
American Museum of Natural History

Recommended Citation
Joel H. Kastner et al 2008 ApJ 672 957 https://doi.org/10.1086/523890

Submitted to *The Astrophysical Journal (Letters)*

Serendipitous *Chandra* X-ray Detection of a Hot Bubble within the Planetary Nebula NGC 5315

Joel H. Kastner[1]

and

Rodolfo Montez, Jr.

Chester F. Carlson Center for Imaging Science, Rochester Institute of Technology, 54 Lomb Memorial Dr., Rochester, NY 14623

jhk@cis.rit.edu, rxm9447@cis.rit.edu

Bruce Balick

Department of Astronomy, University of Washington, Seattle, WA 98195–1580

balick@astro.washington.edu

and

Orsola De Marco

Department of Astrophysics, American Museum of Natural History, Central Park West at 79th Street, New York, NY 10024

orsola@amnh.org

ABSTRACT

We report the serendipitous detection of the planetary nebula NGC 5315 by the *Chandra* X-ray Observatory. The *Chandra* imaging spectroscopy results indicate that the X-rays from this PN, which harbors a Wolf-Rayet (WR) central star, emanate from a $T_X \sim 2.5 \times 10^6$ K plasma generated via the same wind-wind collisions that have cleared a compact ($\sim$ 8000 AU radius) central cavity within the nebula. The inferred X-ray luminosity of NGC 5315 is $\sim 2.5 \times 10^{32}$ erg s^{-1} (0.3-2.0 keV), placing this object among the most luminous such "hot bubble" X-ray sources yet detected within PNe. With the X-ray detection of NGC 5315, objects with WR-type central stars now constitute a clear majority

of known examples of diffuse X-ray sources among PNe; all such "hot bubble" PN X-ray sources display well-defined, quasi-continuous optical rims. We therefore assert that X-ray-luminous hot bubbles are characteristic of young PNe with large central star wind kinetic energies and closed bubble morphologies. However, the evidence at hand also suggests that processes such as wind and bubble temporal evolution, as well as heat conduction and/or mixing of hot bubble and nebular gas, ultimately govern the luminosity and temperature of superheated plasma within PNe.

Subject headings: planetary nebulae: general — planetary nebulae: individual (NGC 5315) — stars: winds, outflows — stars: Wolf-Rayet — X-rays: ISM

1. Introduction

Imaging spectroscopy of planetary nebulae (PNe) by the *Chandra* and *XMM-Newton* X-ray observatories has yielded a steadily accumulating body of compelling observational evidence for "hot bubbles" within certain PNe. Such a hot bubble may be produced as the central star makes the transition from post-asymptotic giant branch (post-AGB) star to white dwarf, following an evolutionary track of increasing $T_\star$ at constant $L_\star$, followed by decreasing $L_\star$ and $T_\star$. In this phase the star produces very fast and energetic winds (with speeds ~ 1000 km s^{-1} and mass loss rates $\gtrsim 10^{-7}$ $M_\odot$ yr^{-1}). When such a fast wind collides with ambient (previously ejected AGB) gas, it is shocked and superheated (e.g., Zhekov & Perinotto 1996). The shocked fast wind forms an overpressured bubble that accelerates outwards and displaces the ambient (visible, nebular) gas as it grows (Kwok, Purton, & Fitzgerald 1978). The supersonic growth of the bubble plows the displaced older material into a rim of dense gas which, when projected on the sky, is seen as a thin molecular, dust, and/or ionized structure that traces the bubble's perimeter.

So far, nine of ~ 25 PNe targeted by *Chandra* or *XMM* have been detected as diffuse X-ray sources (Kastner et al. 2000, 2001, 2003; Chu et al. 2001; Guerrero et al. 2002, 2005; Sahai et al. 2003; Montez et al. 2005; Gruendl et al. 2006). In most of these nebulae, the X-ray-emitting region is fully contained within bright optical rims or bubbles, as predicted by the preceding "hot bubble" scenario. Furthermore, many of the detected objects harbor central stars that are of Wolf-Rayet (WR) type (i.e., "[WC]" or "[WO]" stars) and/or display optical

[1]Visiting Astronomer, Laboratoire d'Astrophysique de Grenoble, Université Joseph Fourier — CNRS, BP 53, 38041 Grenoble Cedex, France

spectroscopic evidence for large mass-loss rates and wind velocities. In this *Letter*, we report the serendipitous detection by *Chandra* of X-ray emission associated with an additional [WC] PN, NGC 5315, and we present evidence that this emission also arises within a hot bubble. The accidental detection of NGC 5315 underscores certain trends that are emerging from X-ray detections of PN hot bubbles over the past decade.

2. X-ray Detection of NGC 5315

In a Cycle 5 Chandra study, we observed two [WC] PNs, NGC 40 and Hen 2-99; we detected the former, but failed to detect the latter (Montez et al. 2005). Recently, while searching the Chandra archives for targeted observations of PNs, one of us (Montez) established that a *second* [WC] PN, NGC 5315 (Fig. 1), was present in the 29 ks Chandra Advanced CCD Imaging Spectrometer (ACIS) observation that targeted Hen 2-99 (OBSID 4480). The position of NGC 5315 lies just within the field of view of the ACIS-S detector array, on a CCD (the front-illuminated S4) that lies adjacent to the prime imaging CCD (the back-illuminated S3). Examination of the Chandra/ACIS image revealed an X-ray source at the position of NGC 5315, $\sim 12.5'$ off-axis (Fig. 2).

Due to the large off-axis angle and the fact that — when not used in conjunction with the high-energy transmission gratings — ACIS-S4 deviates significantly from the focal surface of the Chandra mirror assembly, the NGC 5315 X-ray source is subject to severe image aberrations. The Chandra PSF semimajor axis is $\sim 10 - 20''$ at such off-axis angles[2], without accounting for the displacement of the S4 detector from the focal surface. Hence, apart from establishing that an X-ray source is coincident with the position of NGC 5315, no spatial information can be readily extracted from the ACIS-S4 image.

We used version 3.4 of CIAO[3] to extract source and background spectra, spectral responses, and light curves. The circular source extraction region radius was $34''$ (Fig. 2), which should encompass the 95% encircled energy of a point source at the off-axis angle corresponding to the position of NGC 5315. Background was extracted from a $\sim 2.5' \times 3.5'$ rectangular region adjacent to the NGC 5315 source (Fig. 2). The resulting, background-subtracted spectrum displays prominent Ne IX emission at ~ 0.9 keV and a blend of O VII and O VIII emission lines at ~ 0.65 keV (Fig. 3).The background-subtracted count rate of the source is 12.4 ± 0.7 ks^{-1}. The light curve (not shown) reveals no significant variation in

[2]See e.g. http://cxc.harvard.edu/ccw/proceedings/02_proc/presentations/c_allen/offaxis_psf.pdf.gz

[3]http://cxc.harvard.edu/ciao/

this count rate during the 28.7 ks exposure.

3. Spectral Modeling

We used version 12.3.0 of XSPEC[4] (Arnaud 1996) to fit absorbed thermal plasma emission models to the NGC 5315 X-ray source (Fig. 3). The model absorbing column was fixed at $\log N_H(\mathrm{cm}^{-2}) = 21.36$, corresponding to the measured extinction toward NGC 5315 ($A_V \approx 1.3$; Peimbert et al. 2004; Pottasch et al. 2002; Cahn et al. 1992). Applying the VMEKAL variable-abundance plasma emission model (Liedahl et al. 1995 and references therein), we find the best-fit plasma temperature is $T_x = 2.6 \times 10^6$ K ($\pm 10\%$) and the inferred intrinsic X-ray luminosity is $L_x \sim 2.6 \times 10^{32}$ erg s^{-1} (0.3–2.0 keV) assuming a distance[5] of 2.5 kpc (Marcolino et al. 2007). The plasma modeling suggests Ne is enhanced and Fe is depleted; the best-fit VMEKAL model abundances are 4.3 ± 1.3 and 0.6 ± 0.3, respectively, relative to solar (Anders & Grevesse 1989).

4. Discussion

Due to the very poor off-axis *Chandra*/ACIS-S image quality at the position of NGC 5315, it is not possible to ascertain from the ACIS image alone whether the X-rays trace a hot bubble within this PN, emanate from the PN nucleus, or are emitted by both the nebula and its central star(s). However, the background-subtracted spectrum (Fig. 3), the luminosity, and the temporal behavior of the X-ray source associated with NGC 5315 appear quite definitive regarding the origin of the X-rays. The spectrum shows strong Ne IX line emission as well as a blend of O VII and O VIII lines, with no evidence for Fe L-shell lines. Spectral modeling indicates that the emission arises in a ~ 2.5 MK thermal plasma with enhanced Ne and depleted Fe. These results and the inferred source L_X are very similar to those obtained for the best-characterized diffuse X-ray PN, BD +30°3639 (Kastner et al. 2000, 2006; Maness et al. 2003). Meanwhile, the Chandra/ACIS light curve shows no evidence for variability, and the absorption-corrected X-ray luminosity of NGC 5315 is at least an order of magnitude larger than that of any unresolved PN core region detected thus far (Guerrero et al. 2001; Kastner et al. 2003), further supporting the interpretation that the X-rays arise from an extended region within NGC 5315.

---

[4]http://heasarc.nasa.gov/docs/xanadu/xspec/

[5]Estimates of the distance to NGC 5315 range from ∼1.3 kpc (Cahn et al. 1992; Pottasch 1982) to 2.6 kpc (Gathier et al. 1986).

Assuming the X-rays from NGC 5315 indeed arise from its compact ($\sim 1''$ radius), sharply delineated central cavity (Fig. 1), the results reported here establish NGC 5315 as one of the most luminous "hot bubble" X-ray sources yet detected (Table 1). The detection of NGC 5315 by *Chandra* therefore underscores three significant trends that have emerged from the X-ray observations of PNe obtained thus far by *Chandra* and *XMM*:

1. Objects with WR-type (i.e., [WC], [WO], or WR(H)) central stars — which display characteristically large wind velocities (v_w), large mass-loss rates ($\dot{M}$), and relatively low effective temperatures ($T_{\rm eff} \sim 30 - 60$ kK; e.g., Crowther et al. 1998) — account for five of the seven detections of "hot bubble" (as opposed to jet-excited) PN X-ray sources (Table 1). Given that $\lesssim 10\%$ of galactic PNe are known to harbor WR-type central stars (Gorny & Stasinska 1995; Tylenda 1996), such PNe (and [WC] PNe in particular) clearly constitute a disportionately large fraction of objects that are established sources of luminous, diffuse X-ray emission. One of the two PNe in Table 1 that does not have a WR-type central star, NGC 7009, displays a very large central star wind velocity. The only X-ray nondetection among the [WC] PNe, the cool ([WC 9]) and very young Hen 2-99, appears to contain a bright, compact core, and hence may not yet have formed a central, wind-blown bubble (Montez et al. 2005).

2. All of the Table 1 objects — not just the WR-type PNe — feature central stars that are relatively cool and luminous ($T_{\rm eff} \lesssim 80$ kK and $L \sim 3000 - 10000\ L_{\odot}$; e.g., Mal'Kov 1997) confirming that PNe with X-ray-luminous bubbles are quite young (Soker & Kastner 2003) and suggesting such PNe are generally the descendants of relatively massive progenitors. Specifically, comparison with theoretical post-AGB evolutionary tracks (e.g., Fig. 1 of Perrinoto et al. 2004) suggests post-AGB ages $\lesssim 3000$ yr (in general agreement with the dynamical ages of these PNe; see, e.g., Fig. 7 of Akashi et al. 2006) and progenitor masses in the range $1 - 5\ M_{\odot}$.

3. In all cases in which diffuse X-ray emission is detected, the optical/IR structures that enclose the regions of diffuse X-rays are clearly defined, and these structures generally display thin, bright, uninterrupted edges (or "rims") surrounding a cavity of lower surface brightness that is coincident with the extended X-ray emission (see also Gruendl et al. 2006).

In Fig. 4 we display scatter diagrams for various of the observed quantities listed for the X-ray-detected PNe in Table 1. The top panels of Fig. 4 demonstrate that the characteristic temperature of the X-ray-emitting plasma is far lower than expected, based on simple shock models, in almost all PNs in which diffuse X-ray emission has been detected thus far (consistent with the early X-ray CCD spectroscopic results reported for BD +30°3639 by

Arnaud et al. 1996). The heat generated by stellar wind shocks should produce a post-shock temperature $T = 2.5 \times 10^6 (v_w/400)^2$ (where v_w is in km s^{-1}; e.g., Stute & Sahai 2006 and references therein). There is only one Table 1 object, NGC 2392, for which the temperature so predicted is consistent with T_X; for all other PNe, the predicted post-shock temperatures are larger than observed by factors ranging from ~ 2 (BD +30°3639) to ~ 200 (NGC 7026). Furthermore, T_X appears uncorrelated with present-day central star wind velocity, but is weakly anticorrelated with PN bubble radius (Fig. 4, upper panels), suggesting that PN age is more important than present-day wind kinetic energy in determining the temperature of the X-ray-emitting plasma.

The bottom panels of Fig. 4 indicate that X-ray luminosity is correlated with present-day central star wind luminosity $L_w = \frac{1}{2}\dot{M}v_w^2$, and is perhaps anticorrelated with bubble radius. In the L_X vs. L_w plot (Fig. 4, lower left), NGC 40 appears somewhat underluminous in X-rays relative to the other PNe, consistent with the "punctured" appearance of its central bubble (Montez et al. 2005 and references therein). The shallow slope of the L_X vs. L_w correlation — wherein 4 orders of magnitude in L_w results in only a factor ~ 20 range in L_X — may suggest either that the conversion of wind kinetic energy to plasma radiation becomes more efficient as the central star wind declines in strength, or that the luminosities (and, perhaps, temperatures) of the hot bubbles within these PNe are established during early phases of the post-AGB evolution of central stars with rapidly evolving winds (Akashi et al. 2006, 2007).

5. Conclusions

We have detected luminous ($L_X \sim 2.5 \times 10^{32}$ erg s^{-1}), soft ($T_X \sim 2.5 \times 10^6$ K) X-ray emission from the [WC] PN NGC 5315. The emission most likely emanates from a relatively compact (~ 8000 AU radius), wind-blown bubble within this PN. Placed in the context of results obtained to date by *Chandra* and *XMM*, these results for NGC 5315 indicate that the combination of (1) relatively young, massive PNe harboring central stars with large wind kinetic energies ($L_w \gtrsim 10^{33}$ erg s^{-1}) and (2) a "closed containment vessel" is necessary to yield PN hot bubbles with plasma densities sufficient to produce detectable soft (0.3-2.0 keV) X-ray luminosities $L_X \gtrsim 10^{31}$ erg s^{-1}. There should exist many other examples of diffuse, "hot bubble" X-ray emission in addition to those listed in Table 1, particularly among [WC] PNe with large "present-day" central star wind luminosities and "closed" bubble/lobe morphologies. A systematic *Chandra* and *XMM* survey of such PNe as well as a set of "control" objects — in particular, [WC] PNe with open/amorphous morphologies on the one hand, and PNe with low-L_w central stars but closed, bubble-like structures on the other

— would test these assertions. In addition, to determine the longevity of X-ray-luminous hot bubbles, it is important to search for X-ray emission from the descendants of [WC] PNe, i.e., PNe with PG 1159-type central stars. In this regard, it is intriguing that two such objects, K 1–16 and NGC 246 (Jeffery et al. 1996), apparently have gone undetected by *Chandra*[6].

Collectively, these results provide further motivation for ongoing modeling efforts that attempt to incorporate processes such as the early onset (and rapid decline) of the central star's fast wind, adiabatic cooling of the (expanding) hot bubble, and heat conduction between the shocked wind and nebular gas in predicting the range and evolution of L_X and T_X in PNe (see discussions in Soker & Kastner 2003; Akashi et al. 2006, 2007; Stute & Sahai 2006; Schönberner et al. 2006). Additional, detailed modeling of a much larger and more representative database of X-ray observations of PNe will be required to establish which (if any) of the above processes are particularly significant in determining L_X and T_X within PN hot bubbles.

This research was supported by NASA through Chandra awards GO4–5169X and GO5–6008X issued to Rochester Institute of Technology by the Chandra X-ray Observatory Center, which is operated by Smithsonian Astrophysical Observatory for and on behalf of NASA under contract NAS8–03060. The authors wish to acknowledge important contributions to (and comments on) this paper by Noam Soker.

CXO(ACIS)

REFERENCES

Akashi, M., Soker, N., & Behar, E., 2006, MNRAS, 368, 1706

Akashi, M., Soker, N., & Behar, E., 2007, MNRAS, 375, 137

Anders, E., & Grevesse, N. 1989, Geo. Cos. Acta, 53, 197

Arnaud, K., 1996, Astronomical Data Analysis Software and Systems V, eds. Jacoby G. & Barnes, J., p. 17, PASP Conf. Series Vol. 101

Arnaud, K., Borkowski, K.J., Harrington, J.P., 1996, ApJ, 462, L75

Cahn, J.H., Kaler, J.B., & Stanghellini, L.et al. 1992, A&AS, 94, 399

[6]Based on preliminary analysis of archival data; see http://www.iaa.es/xpn/.

Chu, Y.-H., Guerrero, M.A., Gruendl, R.A., Williams, R.M., & Kaler, J.B., 2001, ApJ, 553, L69

Crowther, P. A., De Marco, O., & Barlow, M. J. 1998, MNRAS, 296, 367

Gathier R., Pottasch S.R., & Pel J.W. 1986, A&A, 157, 171

Gorny, S. K., & Stasinska, G. 1995, A&A, 303, 893

Gruendl, R.A., Guerrero, M.A., Chu, Y.-H., Williams, R.M. 2006, ApJ, 653, 339

Guerrero, M.A., Chu, Y.-H., Gruendl, R.A., Williams, R.M., & Kaler, J.B., 2001, ApJ, 553, L55

Guerrero, M.A., Chu, Y.-H., & Gruendl, R.A., 2002, A&A, 387, L1

Guerrero, M.A., Chu, Y.-H., Gruendl, R. A., & Meixner, M. 2005, A&A, 430, L69

Hyung, S., & Feibelman, W. A. 2004, ApJ, 614, 745

Jeffery, C.S., Heber, U., Hill, P.W., Dreizler, S., Drilling, J.S., Lawson, W.A., Leuenhagen, U., & Werner, K. 1996, in *Hydrogen deficient stars*, ASP Conf. Ser., Vol. 96, eds. C. S. Jeffery & U. Heber, p. 471

Kastner, J.H., Soker, N., Vrtilek, S.D., & Dgani, R., 2000, ApJ, 545, L57

Kastner, J.H., Vrtilek, S.D., Soker, N., 2001, ApJ, 550, L189

Kastner, J.H., Balick, B., Blackman, E.G., Frank, A., Soker, N., Vrtilek, S.D., Jingqiang, Li, 2003, ApJ, 591, L37

Kastner, J.H., Yu, Y.S., Houck, J., Behar, E., Nordon, R., & Soker, N. 2006, in *Planetary Nebulae*, Proc. IAU Symp. 234, eds. Barlow & Mendez (Camb. U. Press), p. 169

Koesterke, L., & Hamann, W.-R. 1997, in *Planetary Nebulae*, Proc. IAU Symp. 180, eds. H. J. Habing & H. J. G. L. M. Lamers (Dordrecht: Kluwer)

Kwok, S., Purton, C.R., & Fitzgerald, P.M. 1978, ApJ, 219, L125

Leuenhagen, U., Hamann, W.-R., Jeffery, C.S., 1996, A&A, 312, 167

Liedahl, D.A., Osterheld, A.L., & Goldstein, W.H. 1995, ApJL, 438, 115

Mal'Kov, Yu.F. 1997, ARep, 41, 760

Maness, H.L., Vrtilek, S.D., Kastner, J.H., & Soker, N. 2003, ApJ, 589, 439

Marcolino, W.L.F., Hillier, D.J., de Araujo, F.X. & Pereira, C.B. 2007, ApJ, 654, 1068

Montez, R., Kastner, J.H., De Marco, O., Soker, N. 2005, ApJ, 635, 381

Peimbert, M., Peimbert, A., Ruiz, M. T., & Esteban, C., 2004, ApJS, 150, 431

Perinotto, M. 1993, in *Planetary Nebulae*, Proc. IAU Symp. 155, eds. R. Weinberger & A. Acker (Kluwer), p. 57

Perinotto, M., Cerruti-Sola, M., & Lamers, H. J. G. L. M. 1989, ApJ, 337, 382

Perinotto, M., Schönberner, D., Steffen, M., & Calonoci, C. 2004, A&A, 414, 993

Pottasch, S.R. 1982, in *Planetary Nebulae*, Proc. IAU Symp. 103, ed. D.R. Flower, p. 391

Pottasch, S.R., Beintema, D. A., J. Bernard Salas, J., Koornneef, J., Feibelman, W. A., 2002, A&A, 393, 285-294)

Sahai, R., Kastner, J.H., Frank, A., Morris, M., & Blackman, E. G. 2003, ApJ, 599, L87

Schönberner, D., Steffen, M., & Warmuth, A. 2006, in *Planetary Nebulae*, Proc. IAU Symp. 234, eds. Barlow & Mendez (Camb. U. Press), p. 161

Soker, N. & Kastner, J.H., 2003, ApJ, 583, 368

Stute M., & Sahai, R. 2006, ApJ, 651, 882

Tinkler, C. M., & Lamers, H. J. G. L. M. 2002, A&A, 384, 987

Tylenda, R. 1996, in *Hydrogen deficient stars*, ASP Conf. Ser., Vol. 96, eds. C. S. Jeffery & U. Heber, p. 101

Zhekov, S.A., & Perinotto, M. 1996, A&A, 309, 648

Table 1. Properties of Diffuse X-ray Planetary Nebulae[a]

Object	Sp. type	D (kpc)	V_w (km s^{-1})	dM/dt ($M_\odot$ yr^{-1})	R_B[b] (pc)	L_X (10^{32} ergs s^{-1})	T_X (10^6 K)
NGC 7026	[WO 3] (1)	1.7 (3)	3500 (6)	4.6×10^{-7} (6)	0.062	4.5 (7)	1.1 (7)
NGC 5315	[WC 4] (1)	2.5 (4)	2400 (4)	1.5×10^{-6} (4)	0.038	2.6 (8)	2.6 (8)
BD +30°3639	[WC 9] (1)	1.2 (4)	700 (4)	1.6×10^{-6} (4)	0.023	2.3[c] (9)	2.2 (10)
NGC 6543	Of/WR(H) (2)	1.8 (2)	1900 (2)	4.0×10^{-8} (2)	0.083	1.0 (11)	1.7 (11)
NGC 40	[WC 8] (1)	1.4 (4)	1000 (4)	1.8×10^{-6} (4)	0.12	0.40[d] (12)	1.0 (12)
NGC 7009	O(H) (2)	1.6 (2)	2770 (2)	2.8×10^{-9} (2)	0.11	0.30 (13)	1.8 (13)
NGC 2392	Of(H) (2)	0.9 (2)	420 (2)	$< 3.0 \times 10^{-8}$ (2)	0.10	0.26 (14)	2.0 (14)
Hen 2-99	[WC 9] (1)	2.5 (5)	900 (5)	2.6×10^{-6} (5)	··· [e]	< 0.05 (12)	···

[a]Does not include the PNe NGC 7027, Menzel 3, and Hen 3-1475, whose X-ray-emitting regions are likely generated by collimated winds or jets (Kastner et al. 2001, 2003; Sahai et al. 2003). A hot bubble was also detected within NGC 3242 by XMM (see http://www.iaa.es/xpn/), but results for L_X and T_X are not yet available. References for spectral type of PN central star, adopted PN distance (D), PN central star wind velocity (V_w) and mass loss rate (dM/dt), and PN X-ray luminosity (L_X) and temperature (T_X) are listed in parentheses.

[b]Radius of central bubble, based on data reported in Cahn et al. 1992. In most cases, values of R_B have been rescaled based on the adopted PN distances in column 3.

[c]L_X for BD +30°3639 has been rescaled based on the revised distance estimate of 1.2 kpc.

[d]L_X for NGC 40 has been revised upwards from that reported in Montez et al. (2005) as a consequence of model fitting of reprocessed data; the fit results indicate that we had previously not properly accounted for ACIS contamination (http://cxc.harvard.edu/ciao/threads/aciscontam/).

[e]In ground-based optical imaging, Hen 2-99 displays a compact core and $\sim 10''$ radius halo (Montez et al. 2005).

References. — 1. Crowther et al. 1998; 2. Tinkler & Lamers 2002 and references therein; 3. Hyung & Feibelman 2004; 4. Marcolino et al. 2007; 5. Leuenhagen et al. 1996; 6. Koesterke & Hamann 1997; 7. Gruendl et al. 2006; 8. this paper; 9. Kastner et al. 2000; 10. Kastner et al. 2006; 11. Chu et al. 2001; 12. Montez et al. 2005; 13. Guerrero et al. 2002; 14. Guerrero et al. 2005.

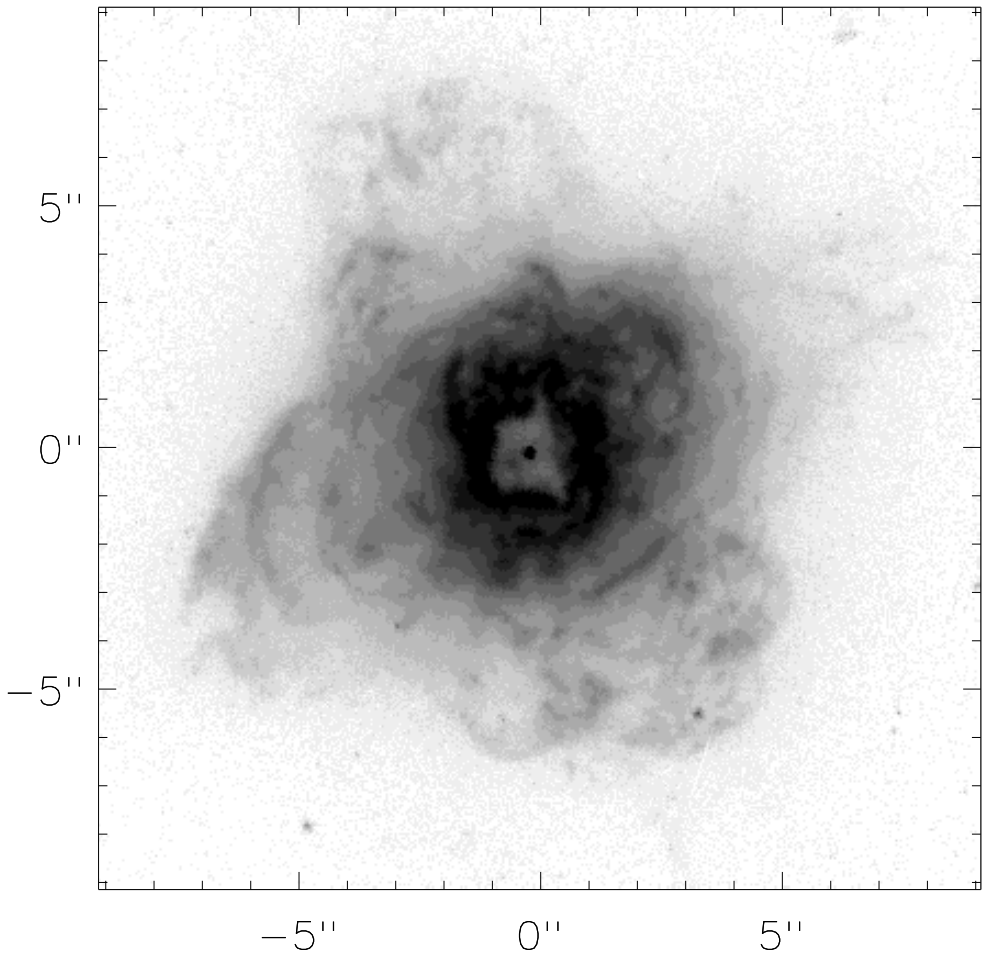

Fig. 1.— *Hubble Space Telescope* WFPC2 Hα (F656N) image of NGC 5315 obtained 2007 February. North is up and east is to the left.

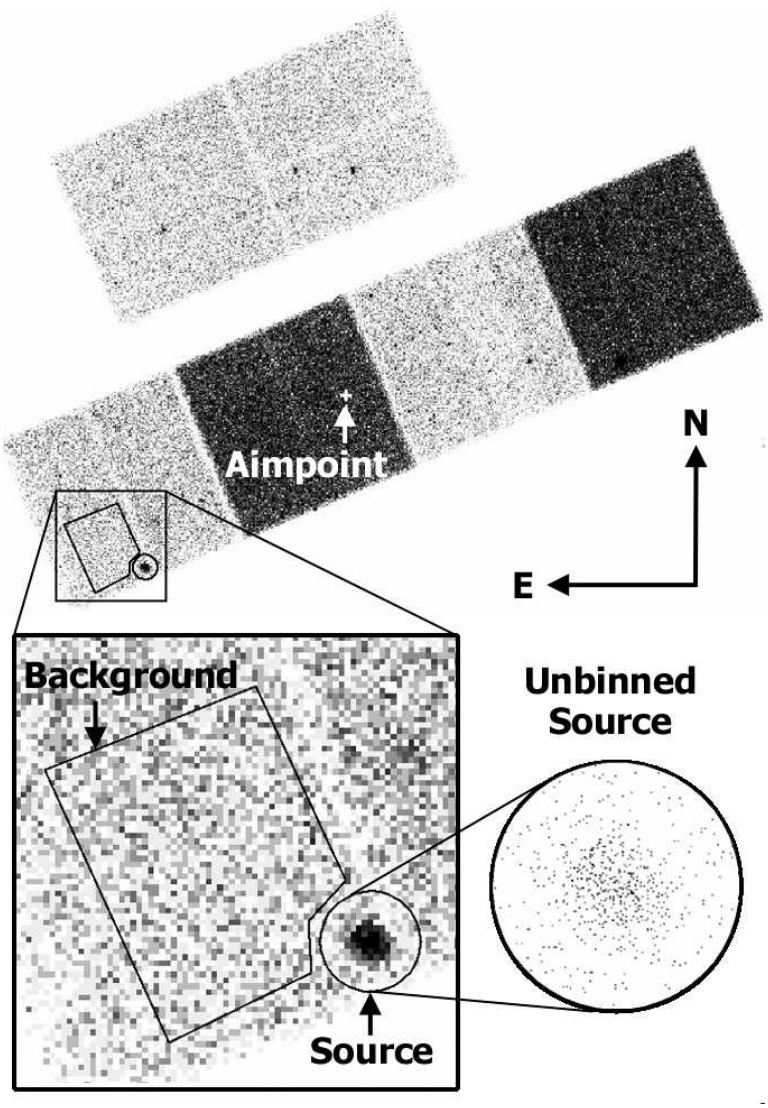

Fig. 2.— Serendipitous Chandra/ACIS observation of NGC 5315. Displayed are rebinned ($3.9'' \times 3.9''$ pixel) images of the entire 6-CCD field (upper half of figure) and a smaller ($5' \times 5'$) region that includes the NGC 5315 X-ray source (lower left), as well as an unbinned ($0.49'' \times 0.49''$ pixel) image of the ($34''$ radius) source spectral extraction region (lower right). The background spectral extraction region is also indicated.

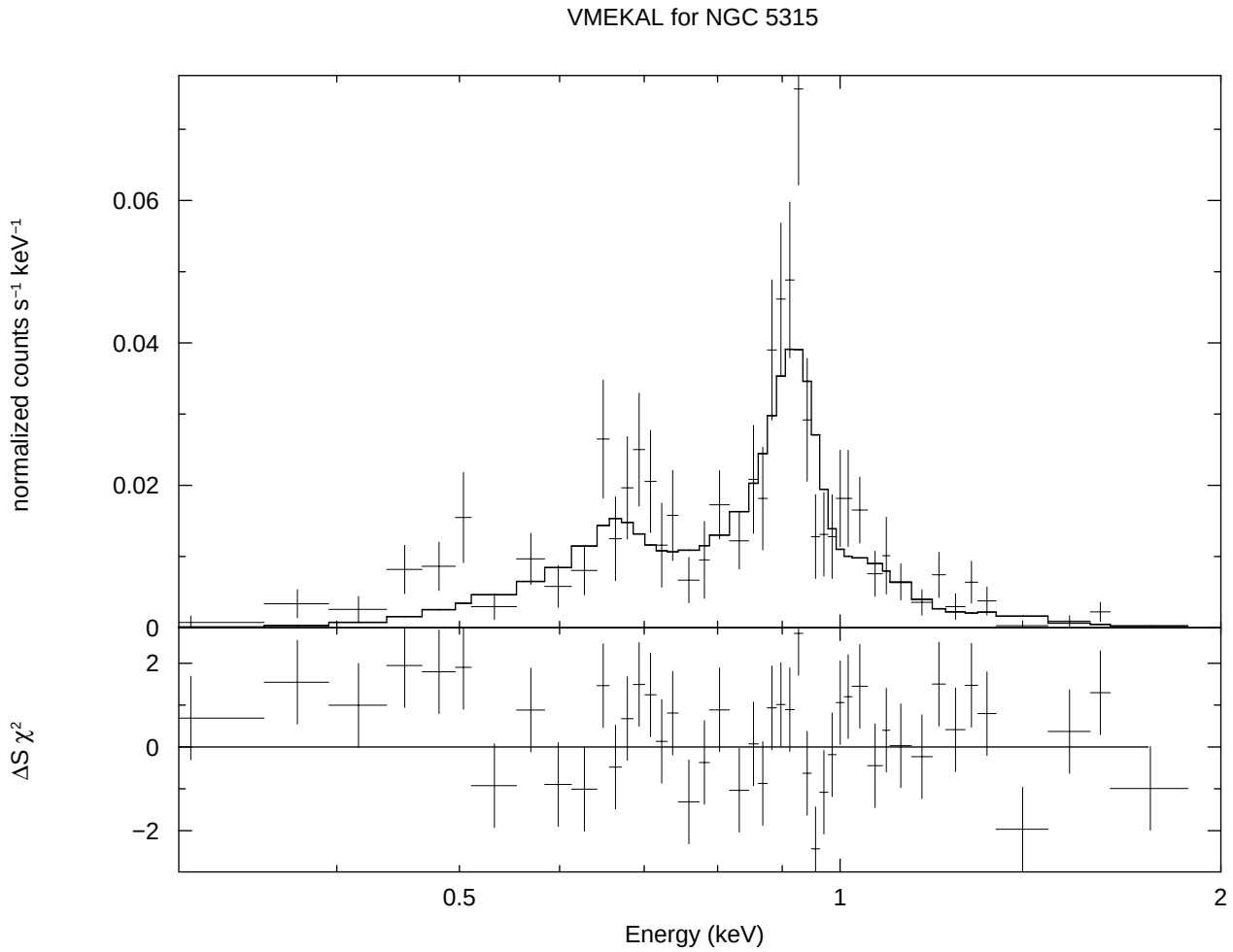

Fig. 3.— Chandra/ACIS spectrum of the X-ray source associated with NGC 5315 (crosses), with best-fit absorbed thermal plasma (VMEKAL) model spectrum overlaid. The fit residuals are indicated in the lower panel.

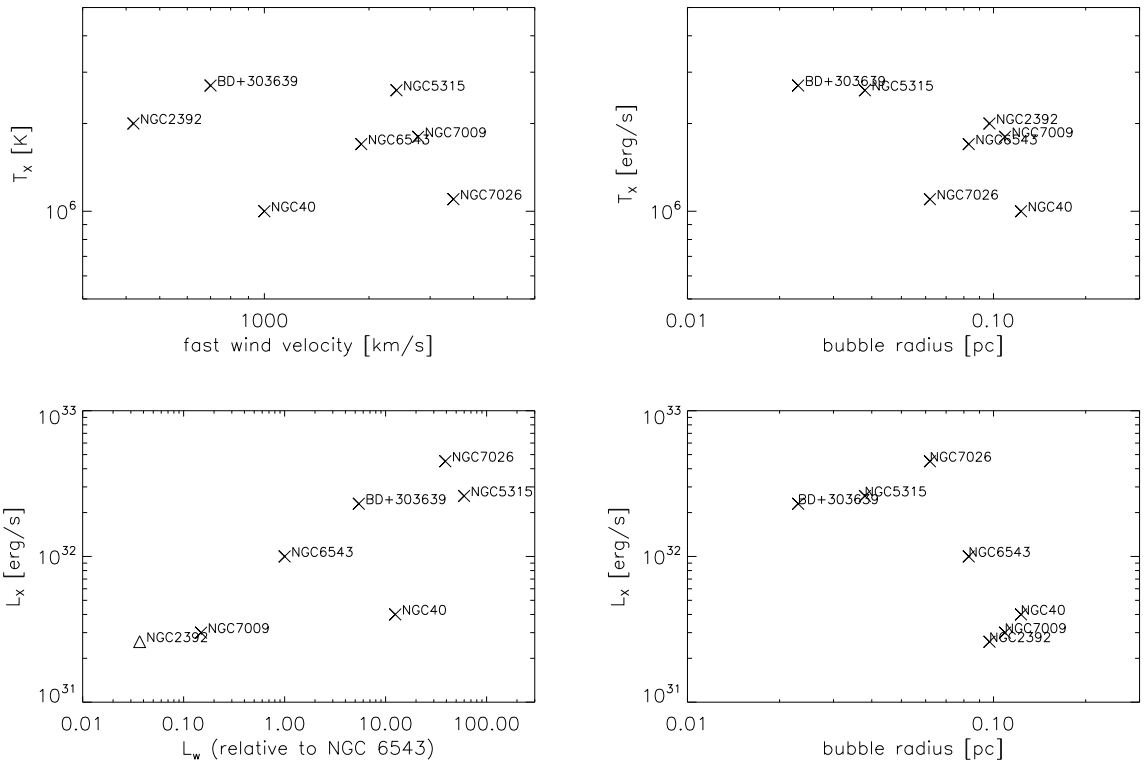

Fig. 4.— Results obtained thus far for PNe detected as "hot bubble" X-ray sources by Chandra and XMM-Newton (Table 1). Upper left: PN plasma temperature (T_X) vs. central star fast wind velocity. Upper right: T_X vs. PN optical bubble radius. Lower left: PN X-ray luminosity (L_X) vs. wind luminosity of the PN central star (L_w) relative to L_w of the central star of NGC 6543 (L_w for NGC 2392 [triangle] is an upper limit). Lower right: L_X vs. PN optical bubble radius.